

## Mechanism for slow waves near cutoff frequencies in periodic waveguides

R. V. Craster,<sup>1</sup> S. Guenneau,<sup>2</sup> and S. D. M. Adams<sup>3</sup>

<sup>1</sup>*Department of Mathematical and Statistical Sciences, University of Alberta, Edmonton, Canada T6G 2G1*

<sup>2</sup>*Department of Mathematical Sciences, Liverpool University, Liverpool L693BX, United Kingdom*

<sup>3</sup>*Department of Mathematics, Imperial College London, London SW72AZ, United Kingdom*

(Received 26 December 2008; published 29 January 2009)

Slow waves are of considerable topical interest; we show that they can be created within a simple waveguiding structure, a planar waveguide with periodic corrugations, and we describe the physical mechanism responsible. We show that this is a general feature of waveguides in both scalar systems, we use the Helmholtz equation within a guide with either Dirichlet or Neumann wall conditions as our main pedagogic example, and in fully coupled systems such as in-plane elasticity. The presence of slow modes within elastic waveguides has remained unexplored and so potential applications have not been exploited. We demonstrate that the same physics is responsible for the elastic slow modes with a subtle nuance connected to the presence of negative group-velocity modes within the elastic system. In addition to describing the mechanism we derive the frequencies at which they arise using a high-frequency asymptotic algorithm. These asymptotics predict the existence of slow modes associated with a countable set of discrete eigenfrequencies around the cutoff frequencies of an unperturbed waveguide. The asymptotic scheme leads to a natural physical explanation for the presence of such slow modes. Finite element computations for both dispersion curves and associated eigenmodes provide further evidence of the existence of slow modes and allow for comparison with the asymptotics. Many new applications are possible, particularly in elasticity, to generate analogies of optical delay lines. Furthermore the guiding structure we describe is simple to construct.

DOI: [10.1103/PhysRevB.79.045129](https://doi.org/10.1103/PhysRevB.79.045129)

PACS number(s): 41.20.Jb, 42.25.Bs, 42.70.Qs, 43.20.+g

There is currently renewed interest in slow waves,<sup>1</sup> also referred to as trapped or frozen modes or localized oscillations depending on the physical context, as detailed in the review.<sup>2</sup> Although commercial applications may not appear immediately, slowed-down light opens vistas in all-optical routers for fiber-optic communication networks. Another exciting potential application lies in the design of the optical equivalent of today's random access memory (RAM) for quantum computing,<sup>3</sup> similar although relatively unexplored applications can be envisaged for systems governed by other wave systems such as in-plane elasticity.

There has been considerable interest and progress in generating slow light using Bragg gratings, fibers, and structured surfaces<sup>4</sup> for which the mechanism is that constructive reflections, relying on periodicity, lead to a path length much longer than the grating length, as discussed in Ref. 5. The mechanism that we shall describe and interpret is not due to periodicity *per se*. Instead we draw upon the literature of localized bound states<sup>6</sup> and trapped modes<sup>7</sup> in quantum rings created by, say, a single defect within an otherwise undeformed and unperturbed waveguide. In these cases the energy decays away from the region of localization. Other related applications such as slow light via population oscillations in quantum well structures are also important.<sup>8</sup> Some recently developed asymptotic methods for trapping mechanisms in curved geometries enable one to reduce the analysis to an ordinary differential equation (ODE) subject to specific effective conditions.<sup>9</sup> Crucially, this also allows for a physical interpretation connected with the fact that these occur at frequencies close to cutoff for the analogous unperturbed guide, and by extending these ideas to a quasiperiodic setting we demonstrate that this creates slow modes.

In this paper, we provide a simple algorithm to generate trapped bound modes in homogeneous, periodic, slowly

varying strips (see Fig. 1) and discuss the physics associated with these slow modes. In this guiding structure we discover that very flat slow modes emerge, which is remarkable: both the asymptotic method and finite element computations identify these modes. The asymptotics lead us to the physics that creates these slow modes. In particular the modes emerge due to the behavior at cutoff frequencies; below these particular frequencies, modes no longer propagate in the straight guide. We focus initially on the case of Neumann boundary conditions,  $\partial\phi/\partial n=0$ , on top and at the bottom of the strip, as this can be used for a unified model of numerous physical examples, including linear water waves in pipelines (with no-flow conditions on walls), water wave channels once the depth dependence has been removed, transverse electric waves in electromagnetic waveguides (infinite conducting boundary conditions are an accurate model for microwaves), and antiplane shear waves in freely vibrating elastic waveguides. However, it is important to note that the phenomena and mechanism we describe also applies to Dirichlet conditions,  $\phi=0$ , on the guide walls. In all cases, the Helmholtz equation governs behavior. The waveguide lies on  $-h < y < h$  and  $-\infty < x < \infty$ , where  $h$  will vary in a prescribed way with distance along the waveguide,  $x$ . Nondimensionalizing length and width with typical half thickness  $\hat{h}$  lead one to

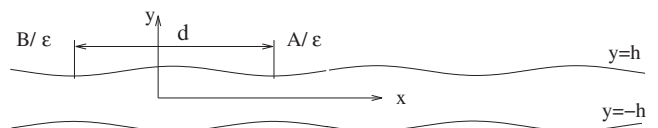


FIG. 1. The periodic waveguide and geometric parameters. In the scalar system we have either Neumann,  $\partial\phi/\partial n=0$ , or Dirichlet,  $\phi=0$ , conditions on the guide walls.

$$\frac{\partial^2 \phi}{\partial x^2} + \frac{\partial^2 \phi}{\partial y^2} + \tilde{\omega}^2 \phi = 0, \quad (1)$$

with  $\tilde{\omega}^2 = \hat{h}^2 \omega^2 / c^2$ , where  $\hat{h}$  is the unperturbed half-guide thickness,  $\omega$  is the angular wave frequency, and  $c$  is the wave speed. This nondimensional frequency  $\tilde{\omega}$  is used henceforth with the tilde decoration dropped. Later we will discuss the in-plane elasticity in which the physics is more involved.

The existence of trapped modes in locally perturbed acoustic waveguides was first observed experimentally by Parker<sup>10</sup> in 1966 with subsequent theoretical calculations of resonance frequencies made the following year.<sup>11</sup> Topographic acoustic and optical waveguides are of considerable interest in applications ranging from delay lines to convolution because of their strong-field confinement features (see Ref. 12 and references therein). The renewed interest comes in particular from recent advances in design of long period grating (LPG) waveguides to achieve better control of the propagation of light, such as reducing its wave speed through ultraflat dispersion at band edges.<sup>13</sup> Here, we analyze a very simple waveguide configuration which is shown to support slow waves at frequencies given by an asymptotic estimate furthering efforts toward ultraslow waves.

We consider periodic topographic variation in the width of the waveguide; that is, we consider a cell of length  $d$  in which a thickness variation is given and this cell periodically repeats in the  $x$  direction (see Fig. 1). The boundary of the guide is defined to be at  $y = \pm h(\epsilon x)$ , where

$$h(\epsilon x) = 1 + \alpha \frac{\epsilon^2}{2} g(\epsilon x) \quad (2)$$

and  $\epsilon$  is a small parameter introduced so that formally the variations are weak. The parameter  $\alpha$  can be positive or negative for a guide thickened or thinned, relative to the unperturbed guide ( $\alpha=0$ ), of thickness two. In the numerical simulations the function  $g(\epsilon x)$  is taken to be Gaussian  $g(\xi) = \exp(-\beta \xi^2)$  with  $\xi = \epsilon x$ , although it could be any smooth function. The cell lies on  $-B/\epsilon < x < A/\epsilon$  and  $-h(\epsilon x) < y < h(\epsilon x)$ , and Bloch conditions hold for  $\phi$  at the left and right ends of the cell as follows:

$$\begin{aligned} \phi(-B, y) \exp(ik_0 d) &= \phi(A, y), \\ \frac{\partial \phi}{\partial \xi}(-B, y) \exp(ik_0 d) &= \frac{\partial \phi}{\partial \xi}(A, y). \end{aligned} \quad (3)$$

Importantly, the Bloch wave number,  $k_0$ , measures the change in phase across the cell. Ultimately dispersion curves of frequency versus the Bloch wave number identify pass and stop bands within the structure, and very flat curves correspond to almost standing waves, which propagate energy very slowly through the structure.

It is not widely appreciated that there is a readily accessible high-frequency asymptotic regime near cutoff. When the guide is perfectly straight there are transverse resonances at  $\omega = n\pi/2$  (for  $k_0 d = 0$ ) and  $\phi(x, y) \sim \cos[n\pi(y+1)/2]$  as cutoff is approached,  $n=0, 1, 2, \dots$ . Perturbing away from these frequencies with

$$\phi = \phi_0 + \epsilon^2 \phi_2 + \dots \quad \text{and} \quad \omega^2 = (n\pi/2)^2 + \epsilon^2 \lambda_2 + \dots \quad (4)$$

gives

$$\phi_0(\xi, y) = f_0(\xi) \cos[n\pi(y+1)/2], \quad (5)$$

and the variation along the cell is governed by  $f_0(\xi)$  that satisfies a differential eigenvalue problem,

$$\frac{d^2 f_0}{d\xi^2} + \alpha g(\xi) \left( \frac{n\pi}{2} \right)^2 f_0 + \lambda_2 f_0 = 0. \quad (6)$$

This approach has been utilized to evaluate the asymptotic structure and eigenstates in closed quantum rings<sup>7</sup> where periodicity, rather than the Bloch quasiperiodicity in Eq. (3), is used. The bound states in a quantum ring arise due to curvature rather than thickness variation, which induces an effective attractive potential.<sup>14</sup> For the ODE [Eq. (6)], one applies Bloch condition (3) with  $f_0$  replacing  $\phi$ , with the  $y$  dependence having been removed. Solving Eq. (6) using a spectral approach yields eigenfrequencies as follows:

$$\omega \sim \sqrt{(n\pi/2)^2 + \epsilon^2 \lambda_2}, \quad (7)$$

and we note that the frequency correction  $\lambda_2$  can be negative, leading to localized states at eigenfrequencies below cutoff. The ODE in Eq. (6) is *identical* in both Dirichlet and Neumann cases, the only change being the leading-order structure across the guide; the cosine above is replaced by sine for the Dirichlet case as in Ref. 15 which treats a different situation—that of striped guides. In this periodic structure we are finding bound states created not by curvature but by thickness variation and quasiperiodicity; these periodic bound states provide the slow wave motion that is observed. Another major point to emphasize is that the procedure and physics described are not low-frequency models but instead are accurate even at high frequencies.

Compared with earlier work published on trapped modes within infinitely long locally perturbed waveguides,<sup>9</sup> we now introduce quasiperiodicity and hence additional components in the wave number (or Bloch parameter). Figure 2 shows the band diagrams resulting from the variation in the wave number  $0 \leq k_0 d \leq \pi$  within the first Brillouin zone for a thickened guide with  $\alpha = +10$ . The folding of modes causes modes to cross, but the small perturbation from a straight guide induces a degeneracy split at the edge  $k_0 d = \pi$  of the Brillouin zone, thus opening stop bands [see Fig. 2(a)]. More interestingly, the same panel displays two apparently flat dispersion curves in the frequency range [1.5, 1.6]. Upon closer inspection [see Fig. 2(b)], in which dispersion curves given by asymptotic formula (7) for  $n=1$  are drawn as solid lines, we observe that the lower flat curve is ultraflattened ( $\partial^2 \omega / \partial^2 k_0 \sim 0$ ), whereas the upper one, which sits neatly within the stop band, displays a negative group velocity  $\partial \omega / \partial k_0 < 0$ . Importantly, both curves are located below the cutoff frequency,  $\omega = \pi/2$ , for the analogous straight guide, suggesting that a localized periodic region embedded within a straight guide would be able to sustain such an excitation with only weak coupling into the surrounding guide through evanescent modes. In panels (c) and (d) dispersion curves given by asymptotic formula (7) for  $n=2$  and  $n=3$  are drawn in solid lines, and we note a larger discrepancy with finite

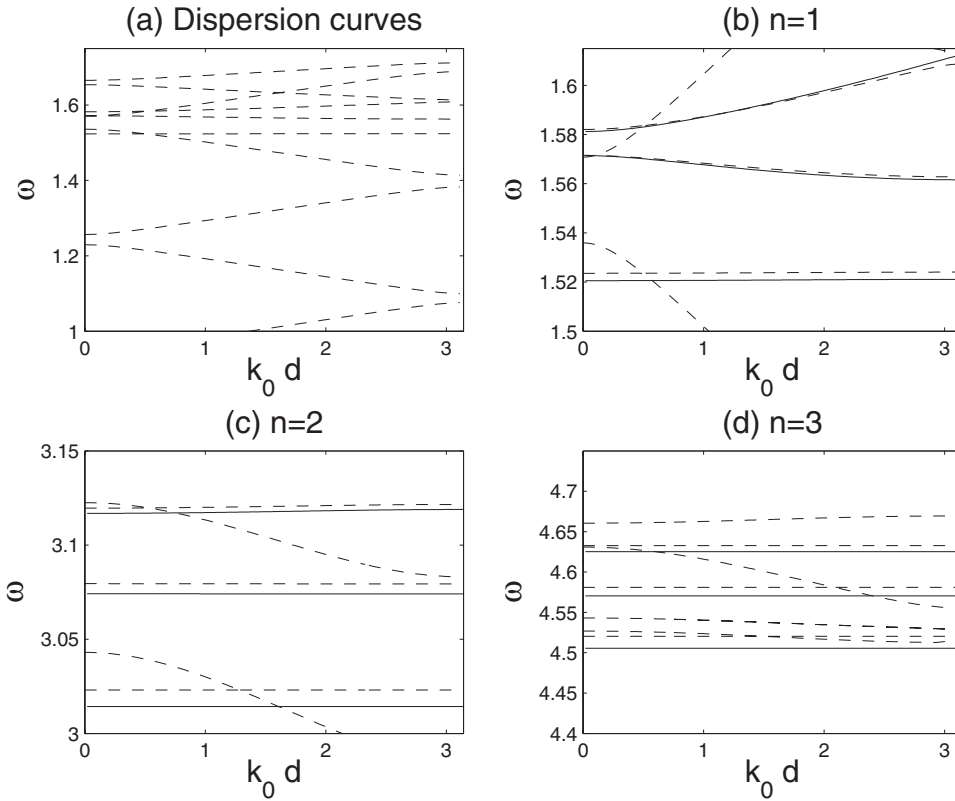


FIG. 2. Dispersion curves for a homogeneous topographic waveguide with height variation given by Eq. (2) with  $-1 < \epsilon x < 1$ ,  $\epsilon = 0.1$ , and  $\alpha = 10$ . Panel (a) shows typical dispersion curves for a range of frequencies. Dashed lines correspond to finite element computations, and solid lines correspond to predictions from asymptotic formula (7) for panels (b)  $n=1$ , (c)  $n=2$ , and (d)  $n=3$ .

element computations, which is attributed to inherent inaccuracy induced by the size of the triangular mesh at these high frequencies (in all computations the number of elements was around 30 000). We observe that all slow modes are now associated with ultraflat curves, with one curve that sits deep

within a stop band in both the lower left and lower right panels. In Fig. 3, we show the analogous results for a thinned guide,  $\alpha < 0$ , and here again remarkable agreement between the computations and asymptotics is found. The major difference is that the trapped mode frequencies now sit above

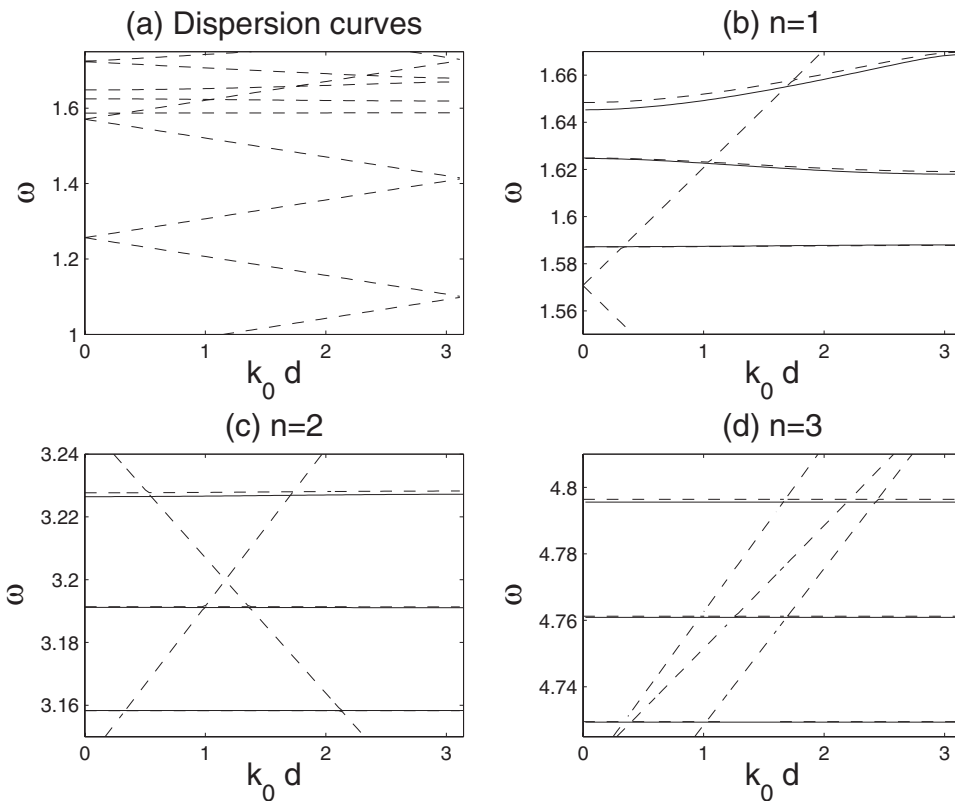


FIG. 3. (a) Dispersion curves for the same values as Fig. 2 but for a thinned guide, with  $\alpha = -10$ . Dashed lines are from finite element computations and solid lines are from Eq. (7) for (b)  $n=1$ , (c)  $n=2$ , and (d)  $n=3$ . In (d) these are completely indistinguishable from the lowest two flat curves predicted by finite elements.

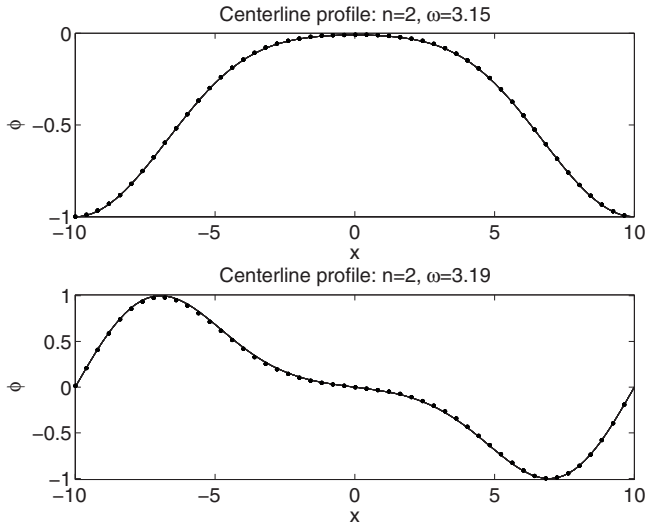


FIG. 4. Mode shapes along the centerline from the asymptotic method (solid lines) and finite elements (dots). These are for the lowest two flat modes, for  $n=2$  and for a thinned guide from Fig. 3(c).

the cutoff frequencies for the analogous straight guide. The asymptotics also produce the mode shapes, two of which are shown and compared to finite element solutions in Fig. 4. The localized modes have their amplitude concentrated in the region of local thickness increase, and again excellent agreement is found with numerics.

We now turn to (isotropic homogeneous) in-plane elasticity. There are again numerous practical examples where slow waves will be valuable, yet the literature on elastic photonics

is much less well developed than in optics—one reason being that elasticity is a fully coupled vector system with both compression and shear waves existing simultaneously and coupling at interfaces. One cannot adopt the equivalent of TE and TM polarizations to decouple them. Nonetheless the asymptotic scheme identifies ODE [Eq. (8)] that governs the near transverse resonance behavior. There are four cases: shear and compression dominated and each is then separated into symmetry and antisymmetry, in  $y$ , about the centerline. There are then four transverse resonance frequencies:<sup>16</sup>  $\omega_0 = (2n-1)/(2\pi), n\pi, n\pi/\gamma, (2n-1)\pi/2\gamma$  with  $\gamma$  as the ratio of shear to compressional wave speeds ( $\gamma=0.4217$  in Fig. 5). The dispersion curves associated with the lowest two transverse resonance frequencies (the shear antisymmetric case,  $\omega = \pi/2, \pi$ ) are shown. Again, in Fig. 5, strikingly flat dispersion curves emerge and for  $n=1$  the asymptotic predictions are virtually indistinguishable from the full computations. At the higher value of  $n$ ,  $n=2$ , there are many more dispersion curves and there is a slight discrepancy of 2% which is visible between the numerics and asymptotics. Nonetheless the flat modes are still picked out by the asymptotic scheme. It is worthwhile noting that the ODE that emerges in the elastic case<sup>17</sup> has yet further physics embedded within it,

$$-C \frac{d^2 f_0}{d\xi^2} + \alpha g(\xi) \omega_0^2 f_0 + \lambda_2 f_0 = 0. \quad (8)$$

The coefficient of the first term,  $-C$ , is given by the near cutoff group velocity<sup>17</sup>  $c_g = -Ck/\omega_0$ , where  $k$  is the dimensionless wave number of the unperturbed mode. Thus whether the mode is trapped beneath or emerges above, the

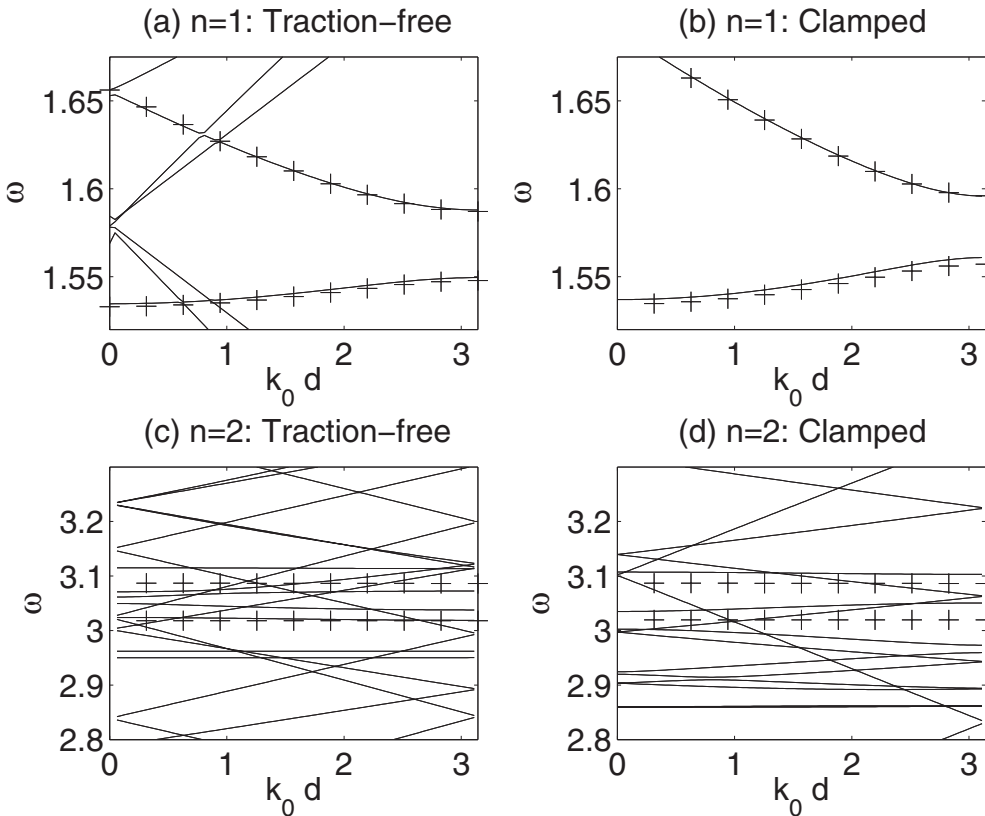


FIG. 5. Dispersion curves near the two lowest transverse resonance frequencies of an elastic waveguide (left: traction-free walls; right: clamped walls). The asymptotics for the slow modes are shown as crosses as, for  $n=1$ , otherwise visually indistinguishable from the finite element dispersion curves (shown as solid lines). The geometrical parameters are the same as in Fig. 2.

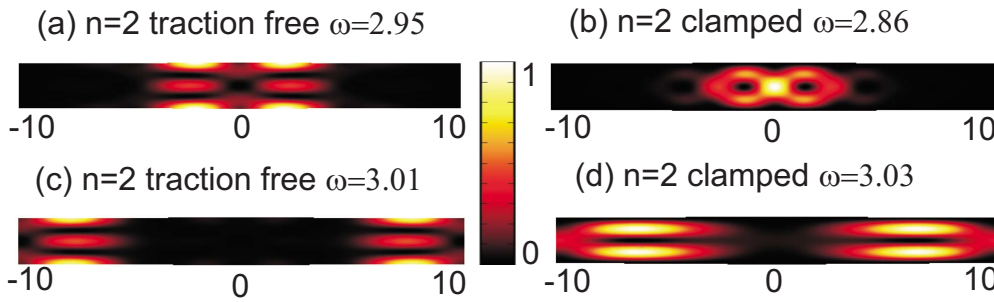


FIG. 6. (Color online) Distribution of energy of slow elastodynamic modes corresponding to panels (c) and (d) of Fig. 5. There is notable similarity between (a) and (c), up to a shift of half a cell.

cutoff frequency depends on the local group velocity. Importantly, for traction-free elastic guides, the second even mode has negative group velocity and this leads to nonintuitive trapping and localization in infinite bent and thickened guides.<sup>17,18</sup> The coefficient  $C$  differs if the boundary conditions change to, say, clamped conditions. Thus the elasticity analogs of Dirichlet and Neumann cases, which are traction-free and clamped cases, no longer share the same ODE. Both cases demonstrate very flat slow modes that are accurately detected by the asymptotic scheme. Figure 5 shows the lowest two, but similar accuracy is detected even at much higher frequencies.

The physical interpretation of the slow modes and the trapping phenomenon, identified here for both acoustics/optics and in-plane elasticity, is that straight guide transverse resonances occur exactly at cutoff frequencies, i.e., the waves simply bounce back and forth across the guide, as can be observed from the lower panel of Fig. 6. Moreover such waves have infinite wavelength in the  $x$  direction despite the

fact that the frequency can be high. Thus near cutoff one is in the nonintuitive position of having high frequency but *long* waves.<sup>16</sup> By perturbing the guide we create additional (periodically located) spaces supporting long waves that are able to propagate at low speed from defect to defect. This mechanism allows very slow waves to propagate through the homogeneous structure. We also note the presence of trapped modes, as shown at the upper panel of Fig. 5, which correspond to the ultraflat bands on panels (c) and (d) of Fig. 5. Given the simple structures that create such slow modes and the prescription we provide to generate the eigenmodes and frequencies, we encourage experimental work to identify and utilize them within delay lines and associated applications in acoustics, optics, and particularly in elasticity. Finally, our results on slow elastic waves suggest a simple design for slow light via stimulated Brillouin scattering, whereby a light pulse can simultaneously be delayed and experience significant amplification in optical fibers.<sup>3,19</sup>

- <sup>1</sup>J. T. Mok, C. Martijn de Sterke, I. C. M. Littler, and B. J. Eggleton, *Nat. Phys.* **2**, 775, (2006).
- <sup>2</sup>A. Figotin and I. Vitebskiy, *Waves Random Complex Media* **16**, 293 (2006).
- <sup>3</sup>J. T. Mok and B. J. Eggleton, *Nature (London)* **433**, 811 (2005).
- <sup>4</sup>T. Baba, *Nat. Photonics* **2**, 465 (2008).
- <sup>5</sup>J. T. Mok, C. Martijn de Sterke, I. C. M. Littler, and B. J. Eggleton *Opt. Photonics News* **18**, 39, (2007).
- <sup>6</sup>P. Duclos, P. Exner, and D. Krejčířik, *Commun. Math. Phys.* **223**, 13 (2001).
- <sup>7</sup>D. Gridin, A. T. I. Adamou, and R. V. Craster, *Phys. Rev. B* **69**, 155317 (2004).
- <sup>8</sup>P. C. Ku, F. Sedgwick, C. J. Chang-Hasnain, P. Palinginis, T. Li, H. Wang, S. W. Chang, and S. L. Chuang, *Opt. Lett.* **29**, 2291 (2004).
- <sup>9</sup>J. Postnova and R. V. Craster, *Wave Motion* **44**, 205 (2007).
- <sup>10</sup>R. Parker, *J. Sound Vib.* **4**, 62 (1966).

- <sup>11</sup>R. Parker, *J. Sound Vib.* **5**, 330 (1967).
- <sup>12</sup>A. A. Oliner, *IEEE Trans. Microwave Theory Tech.* **24**, 914 (1976).
- <sup>13</sup>A. A. Sukhorukov, C. J. Handmer, C. M. de Sterke, and M. J. Steel, *Opt. Express* **15**, 17954 (2007).
- <sup>14</sup>J. T. Londergan, J. P. Carini, and D. P. Murdoch, *Waveguides and Photonic Crystals* (Springer-Verlag, Berlin, 1999).
- <sup>15</sup>S. D. M. Adams, R. V. Craster, and S. Guenneau, *Proc. R. Soc. London, Ser. A* **464**, 2669 (2008).
- <sup>16</sup>J. D. Kaplunov, L. Yu. Kossovich, and E. V. Nolde, *Dynamics of Thin Walled Elastic Bodies* (Academic, New York, 1998).
- <sup>17</sup>D. Gridin, R. V. Craster, and A. T. I. Adamou, *Proc. R. Soc. London, Ser. A* **461**, 1181 (2005).
- <sup>18</sup>J. D. Kaplunov, G. A. Rogerson, and P. E. Tovstik, *Q. J. Mech. Appl. Math.* **58**, 645 (2005).
- <sup>19</sup>M. Gonzalez-Herraez, K. Y. Song, and L. Thevenaz, *Appl. Phys. Lett.* **87**, 081113 (2005).